Pergamon

SCIENCE DIRECT®

Bioorganic & Medicinal Chemistry 11 (2003) 95–103

BIOORGANIC & MEDICINAL CHEMISTRY

Three-Dimensional Pharmacophore Hypotheses of Octopamine/Tyramine Agonists which Inhibit [1-^{14}C]Acetate Incorporation in *Plodia interpunctella*

Akinori Hirashima,[a,*] Tomohiko Eiraku,[b] Yoko Shigeta[c] and Eiichi Kuwano[a]

[a]*Division of Bioresource and Bioenvironmental Sciences, Graduate School, Kyushu University, Fukuoka 812-8581, Japan*
[b]*Graduate School of Bioresource and Bioenvironmental Sciences, Kyushu University, Fukuoka 812-8581, Japan*
[c]*Department of Bioresource and Bioenvironmental Sciences, School of Agriculture, Kyushu University, Fukuoka 812-8581, Japan*

Received 20 May 2002; accepted 5 July 2002

Abstract—Three-dimensional pharmacophore hypotheses were built from a set of 36 octopamine (OA)/tyramine (TA) agonists responsible for the inhibition of sex-pheromone production in *Plodia interpunctella*. Among the ten chemical-featured models generated by a program Catalyst/Hypo, hypotheses including hydrogen-bond acceptor (HBA), hydrogen-bond acceptor aliphatic (HBAl), hydrophobic (Hp), hydrophobic aromatic (HpAr) and hydrophobic aliphatic (HpAl) features were considered to be important and predictive in evaluating OA/TA agonists. Active agonists mapped well onto all the features of the hypothesis such as HBA, HBAl, Hp, HpAr and HpAl features. On the other hand, inactive compounds were shown to be poorly capable of achieving an energetically favorable conformation shared by the active molecules in order to fit the 3-D chemical-feature pharmacophore models. Those hypotheses are considered to be used in designing new leads for hopefully more active compounds. Further research on the comparison of models from the agonists may help elucidate the mechanisms of OA/TA receptor–ligand interactions.

Introduction

Production of the pheromone blend is under the regulation of a neuropeptide termed pheromone biosynthesis activating neuropeptide (PBAN).[1–4] The direct action of PBAN has been demonstrated by studies in vitro[5—10] showing stimulation of pheromone production in the presence of synthetic peptide by isolated pheromone gland tissue. The exact tissue involved was delineated as the intersegmental membrane which is situated between the 8th and 9th abdominal segments.[11,12] In *Helicoverpa armigera*, we have shown that octopamine (OA) and clonidine significantly inhibit the pheromonotropic action due to PBAN in intact moths and decapitated moths, as well as pheromone gland incubations in vitro.[11–13] The inhibition was also reflected in a significant inhibitory effect on intracellular cAMP levels which were stimulated in the presence of PBAN. This inhibitory action is a result of a receptor (separate from the PBAN-receptor) which can be inhibited by pertussis toxin.[12] This provided evidence that this specific pheromonostatic-aminergic receptor is linked to a G-inhibitory protein. Female moths call conspecific males during specific periods when they emit their pheromone. The major pheromone component of Indian meal moth *Plodia interpunctella* was identified as (*Z,E*)-9,12-tetradecadienyl acetate[14–16] and the inhibitors of calling behaviour and pheromone production have been reported.[17]

The biogenic monoamine OA, which has been found in high concentrations in various insect tissues, is the monohydroxylated analogue of the vertebrate hormone noradrenaline. It has been found that OA is present in a high concentration in various invertebrate tissues.[18] This multifunctional and naturally occurring biogenic amine has been well studied and established as: (1) a neurotransmitter, controlling the firefly light organ and endocrine gland activity in other insects; (2) a neurohormone, inducing mobilization of lipids and carbohydrates; (3) a neuromodulator, acting peripherally on

*Corresponding author. Tel.: +81-92-642-2856; fax. +81-92-642-2858; e-mail: ahirasim@agr.kyushu-u.ac.jp

0968-0896/03/$ - see front matter © 2002 Elsevier Science Ltd. All rights reserved.
PII: S0968-0896(02)00320-6

different muscles, fat body, and sensory organs such as corpora cardiaca and the corpora allata, and (4) a centrally acting neuromodulator, influencing motor patterns, habituation and even memory in various invertebrate species.[19,20] The action of OA is mediated through various receptor classes which are coupled to G-proteins and is specifically linked to an adenylate cyclase. Thus, the physiological actions of OA have been shown to be associated with elevated levels of cyclic AMP.[21] Three different receptor classes OAR1, OAR2A and OAR2B have been distinguished from non-neuronal tissues.[22] In the nervous system of locust, a particular receptor class was characterized and established as a new class OAR3 by pharmacological investigations of the [^{3}H]OA binding site using various agonists and antagonists.[23–27] Recently much attention has been directed at the octopaminergic system as a valid target in the development of safer and selective pesticides.[28–30] Structure–activity studies of various types of OA agonists and antagonists were reported using the nervous tissue of the migratory locust, *Locusta migratoria* L.[23–27] However, information on the structural requirements of these OA-agonists and antagonists for OA-receptor ligands with high activity is still limited. Tyramine (TA) showed stronger inhibitory activity (0.63 mM) of pheromone production than that of OA (5.11 mM) in *P. interpunctella*.[17] While it has been clearly shown that OA acts as a neuromediator in various insects, there have only been suggestions that TA might be a neuromediator in invertebrates.[31] Consequently, TA could not only be a biosynthetic precursor to OA, but may also play an independent role as a neuromediator, although it still remains to be clarified. Thus, the pheromonostatic receptor, acting in a neuromodulatory role, represents a novel type of OA/TA receptor. It is therefore of critical importance to provide information on the pharmacological properties of this OA/TA receptor types and subtypes.

Our interest in octopaminergic agonists was aroused by the results of quantitative structure–activity relationships (QSARs) study using various physicochemical parameters as descriptors[32,33] or receptor surface models.[34] Furthermore, molecular modeling and conformational analysis were performed in Catalyst/Hypo[35] to gain a better knowledge of the interactions between octopaminergic antagonists[36] and OAR3 in order to identify the conformations required for binding activity. Similar procedure was repeated using OA agonists.[37] The current work is aimed to generate 3-D chemical function-based hypotheses from some set of OA/TA agonists responsible for the inhibition of sex-pheromone production in *P. interpunctella,* which would identify specific and sensitive inhibitors of pheromone biosynthesis in the future drug design.

Results and Discussion

Assesment of 3-D-QSAR for inhibitory activity

A set of 36 molecules, that are responsible for the inhibition of sex-pheromone production in *P. interpunctella*, was selected as the target training set. Their chemical structures and experimental activities are listed in Figure 1 and Table 1. 2-(Substituted benzylthio)-2-oxazoline (SBO) **4** had the highest potency, followed by SBO derivative **10** and SBO **7**, substituted with 3-CH_3, 4-CH_3 and 3-CF_3, respectively, in inhibition of de novo pheromone production (Table 1). Activities of the agonists

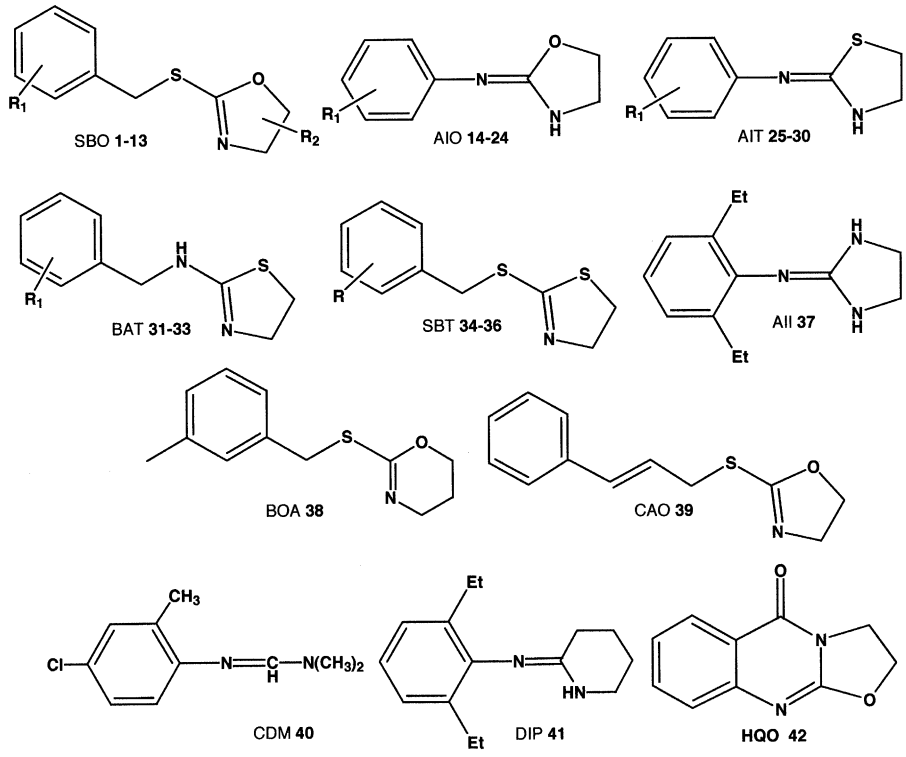

Figure 1. Structures of OA/TA agonists in the training and test sets.

Table 1. OA/TA agonists and their biological activity used in this study

Compd[a]		R1	R2	Mp (°C)	Activity (mM)[b]
1	SBO	H	H	Oil	1.97 (1.15–4.61)
2	SBO	2-CH_3	H	Oil	0.25 (0.19–0.31)
3	SBO	3-Cl	H	Oil	50
4	SBO	3-CH_3	H	Oil	0.088 (0.057–0.153)
5	SBO	3-CH_3	5–CH_3	Oil	0.68 (0.55–0.82)
6	SBO	3-CH_3	4,4′–$(CH_3)_2$	Oil	0.25 (0.19–0.34)
7	SBO	3-CF_3	H	Oil	0.124 (0.082–0.183)
8	SBO	3-CH_3O	H	Oil	0.96 (0.75–1.24)
9	SBO	4-F	H	Oil	0.56 (0.44–0.70)
10	SBO	4-CH_3	H	Oil	0.096 (0.070–0.129)
11	SBO	4-CH_3	4,4′–$(CH_3)_2$	Oil	0.29 (0.22–0.38)
12	SBO	4-CH_3O	H	Oil	0.65 (0.52–0.81)
13	SBO	4-*t*Bu	H	Oil	2.34 (1.25–5.24)
14	AIO	H		132–134	50
15	AIO	2-CH_3		Oil	50
16	AIO	2-CH_2CH_3		61–63	4.67 (3.92–5.56)
17	AIO	2-$CH(CH_3)_2$		89–91	6.46 (5.66–7.35)
18	AIO	2,6-Cl_2		175–176	50
19	AIO	2,6-$(CH_3)_2$		Oil	50
20	AIO	2-CH_3,6-CH_2CH_3		102–104	3.07 (2.14–4.67)
21	AIO	2-CH_3,6-$CH(CH_3)_2$		Oil	5.83 (5.40–6.26)
22	AIO	2,6-$(CH_2CH_3)_2$		172–174	1.65 (1.30–2.05)
23	AIO	2-CH_2CH_3,6-$CH(CH_3)_2$		103–105	0.28 (0.19–0.37)
24	AIO	2,6-$[CH(CH_3)_2]_2$		169–170	1.02 (0.79–1.29)
25	AIT	H		174–176	50
26	AIT	2,4-$(CH_3)_2$		106–108	2.12 (1.82–2.48)
27	AIT	2,4,6-$(CH_3)_3$		99–101	3.03 (2.48–3.65)
28	AIT	2,6-$(CH_3)_2$		169–171	1.38 (1.07–1.75)
29	AIT	2,6-$(CH_2CH_3)_2$		72–74	0.27 (0.18–0.40)
30	AIT	2-CH_2CH_3,6-$CH(CH_3)_2$		138–140	0.82 (0.56–1.15)
31	BAT	2-CH_3		119–120	50
32	BAT	3-CH_3		65–66	2.20 (1.81–2.68)
33	BAT	2,3-$(OCH_3)_2$		102–103	50
34	SBT	2-CH_3		Oil	50
35	SBT	3-CH_3		Oil	50
36	SBT	4-CH_3		Oil	50
37		AII		168–169	4.05 (2.66–6.76)
38		BOA		Oil	0.93 (0.74–1.21)
39		CAO		Oil	1.82 (1.09–3.38)
40		CDM		Oil	3.90 (3.01–4.90)
41		DIP		Oil	50
42		HQO		167–168	50

[a]SBOs **1**–**13** were prepared from oxazolidine-2-thione and substituted benzylamine in the presence of sodium hydride. The compounds reported here have been prepared according to the ref 17. AIOs **14**–**24** were obtained by cyclodesulfurizing the corresponding thiourea with yellow mercuric oxide. AITs **25**–**30** and BATs **31**–**33** were synthesized by cyclization of the corresponding thiourea with concd. Hydrochloric acid. AII **37** was prepared by refluxing the corresponding aniline and 1-acetyl-2-imidazolidone in phosphoryl chloride followed by hydrolysis. BOA **38** was prepared from oxazine-2-thione and *m*-methyl benzylamine in the presence of sodium hydride. CAO **39** were prepared from oxazolidine-2-thione and cinnamylamine in the presence of sodium hydride. DIP **41** was obtained by refluxing δ-valerolactam and the corresponding aniline in phosphoryl chloride. HQO **42** was obtained from SBO and *o*-aminobenzoic acid in the presence of sodium hydride. CDM **40** was a gift from Nihon Nohyaku Co. Ltd. and used after purification by column chromatography on silica gel.

[b]The intersegments of *P. interpunctella* were incubated individually in 10 μL medium containing 0.5 μCi [1-^{14}C]acetate in the presence of synthetic Hez-PBAN (0.5 μM) and test compounds at room temperature for 3 h, maintaining the photoperiod. In order to measure the incorporation of [1-^{14}C]acetate into pheromone components, the glands were extracted in hexane, which was washed with water, and the amount of radioactivity of the hexane extract was measured using a LSC after adding scintillation cocktail. The response obtained in control pheromone gland incubated with Hez-PBAN (0.5 μM) alone is regarded as 100%. The inhibitory activity of OA was 5.11 mM.

are expressed as their ID_{50} values in mM and activities range over three orders of magnitude (min 0.088 mM and max 50 mM). This set included a variety of types of molecules and for this types of training set, the use of the hypothesis generation tool was appropriate. This tool builds hypotheses (overlays of chemical features) for which the fit of individual molecules to a hypothesis can be correlated with the molecule's affinity.

The 3-D-QSAR study was performed with the Catalyst (Version 4.0) package. The geometry of each compound was built with a visualizer and optimized by using the generalized CHARMm-like force field[38–41] implemented in the program. It was found that hypotheses contain good correlation with hydrogen-bond acceptor (HBA), hydrogen-bond acceptor aliphatic (HBAl), hydrophobic (Hp), hydrophobic aromatic (HpAr) and hydrophobic aliphatic (HpAl). The characteristics, such as cost, root mean square (RMS) and the regression constant *r*, of the 10 lowest cost hypotheses are listed in Table 2. The statistical relevance of the various hypotheses obtained is assessed on the basis of their cost relative to the null hypothesis and their *r*.[32] The total fixed cost of the run was 132.37 and the cost of the null hypothesis was

Table 2. Predicted activity (ID_{50}) from 10 best hypotheses against actual inhibitory activity data for 36 OA/TA agonists

Comp.	Exp.[a] (mM)	Conf.[a]	Hypotheses									
			1	2	3	4	5	6	7	8	9	10
1	1.97	10	1.00	0.89	1.10	0.83	0.90	1.00	0.87	0.83	0.78	0.75
2	0.25	18	0.86	0.81	0.72	0.86	0.76	0.89	0.59	0.62	0.78	0.73
4	0.088	29	0.081	0.074	0.078	0.078	0.067	0.083	0.048	0.058	0.074	0.061
5r[b]	0.68	26	0.17	0.20	0.19	0.20	0.15	0.18	0.18	0.15	0.15	0.18
5s[b]	0.68	10	0.57	0.57	1.1	0.58	0.50	0.63	0.93	0.71	0.40	0.54
6	0.25	18	0.093	0.10	0.11	0.11	0.078	0.094	0.072	0.073	0.081	0.085
7	0.12	12	0.18	0.23	0.29	0.26	0.15	0.18	0.22	0.18	0.16	0.20
8	0.96	21	0.36	0.31	0.30	0.29	0.31	0.37	0.32	0.30	0.27	0.25
9	0.56	32	0.89	0.94	0.97	1.00	0.78	0.92	0.79	0.71	0.73	0.80
10	0.096	22	0.51	0.46	0.66	0.43	0.90	0.51	1.30	1.00	0.81	0.92
11	0.29	16	0.36	0.41	0.62	0.42	0.89	0.36	0.97	0.89	0.78	0.83
12	0.65	9	0.26	0.22	0.20	0.21	0.22	0.26	0.22	0.23	0.21	0.19
13	2.34	31	1.10	1.30	1.60	1.40	0.97	1.10	1.30	1.10	0.87	1.00
14	50	2	64	56	53	54	62	65	47	52	53	53
15	50	4	16	14	20	15	15	8.1	17	16	16	12
16	4.7	6	11	10	12	11	10	11	10	9.7	13	7.8
17	6.5	8	9.2	8.0	7.5	7.8	8.5	9.5	6.4	6.8	8.2	7.7
20	3.1	13	1.6	1.6	1.8	1.7	1.4	1.6	2.0	2.3	1.9	1.7
21	5.8	2	2.5	2.3	2.6	2.3	2.3	2.5	3.4	3.7	3.0	2.6
22	1.65	9	1.70	1.50	0.86	1.50	1.50	1.80	0.95	1.10	1.40	1.30
23	0.28	14	2.4	2.2	1.2	2.1	2.2	2.4	1.5	1.7	2.2	2.0
24	1.0	12	3.2	3.2	1.7	3.0	2.8	3.2	2.7	3.0	3.4	3.1
25	50	5	22	48	42	54	21	23	37	41	26	52
26	2.1	4	5.6	4.2	8.4	3.7	5.2	5.9	4.5	3.8	4.1	4.5
27	3.0	2	2.7	2.4	3.5	2.5	2.7	2.9	3.3	3.6	3.0	2.7
28	1.4	7	3.7	3.5	5.3	3.5	4.3	4.0	5.4	5.7	4.8	4.3
29	0.27	11	1.60	1.60	0.93	1.50	1.40	1.60	0.98	1.10	1.40	1.40
30	0.82	7	0.68	1.60	0.90	1.80	0.59	0.70	1.10	1.30	1.10	1.50
31	50	15	12	12	9.1	12	11	13	7.5	7.8	11	11
32	2.2	17	4.3	6.0	7.8	6.2	3.9	4.2	6.1	3.6	3.3	6.3
33	50	20	9.0	7.4	5.8	7.1	8.3	7.5	5.0	5.4	7.7	6.4
37	4.1	25	3.9	3.8	2.9	3.6	3.5	4.2	2.9	3.2	3.4	3.2
38	0.93	38	0.26	0.20	0.21	0.17	1.50	0.26	1.10	1.20	1.0	0.92
39	1.82	4	2.00	1.80	1.10	1.90	1.80	2.00	0.91	0.96	1.70	1.60
40	3.9	4	6.5	4.5	8.7	4.0	6.0	6.7	4.4	6.6	6.0	3.8
42	50	2	63	53	31	54	61	65	61	55	53	54

[a]Exp., experimental data (ID_{50} in mM for inhibition of pheromone production); Conf., number of conformational models.
[b]**5r** has *R* configuration and **5s** *S* configuration.

171.34. The cost range between best hypothesis 1 and null hypothesis was 19.97. The cost range over the 10 generated hypotheses was 2.04. Hypotheses 1 and 2 consist of the same chemical-feature functions as an HBA, an HBAl, an Hp, an HpAl and an HpAr. The Hp of hypotheses 1 and 2 is replaced by an HpAl, leading to hypotheses 5 and 7.

Validation of the hypothesis

The hypotheses are used to estimate the activities of the training set. Those activities are derived from those conformers displaying the smallest RMS deviations when projected onto the hypothesis. Hypotheses 1–10 shared five common features located at almost exactly the same 3-D coordinates. The quality of the correlation among the data in the training set is given by the RMS score which was normalized by the log (uncertainty) and *r*. All calculated activities from 10 best hypotheses and the number of generated conformations for each molecule are listed in Table 2. Even though hypothesis 1 has a lower cost value than others and the RMS index for hypothesis 1 is very small as 0.873, they have nearly no difference in *r* and RMS (Table 3). Roughly speaking, the greater the difference between the cost of the generated hypothesis and that of the null hypothesis, the more likely it is that the hypothesis reflects a chance correlation.[41] The correlation between observed and estimated inhibitory activities is satisfactory in the three hypotheses. The predicted activities are in the right order and parallel the values actually observed (Table 2).

Table 3. Characteristics of 10 lowest cost hypotheses from 36 OA/TA agonists (cost of ideal hypothesis: 132.37, cost of null hypothesis: 171.34)

Hypotheses	Feature[a]					Cost	RMS	*r*
	1	**2**	**3**	**4**	**5**			
1	HBA	HBAl	Hp	HpAl	HpAr	151.37	0.873	0.855
2	HBA	HBA	Hp	HpAl	HpAr	152.05	0.879	0.852
3	HBA	HBAl	Hp	HpAl	HpAr	152.14	0.909	0.841
4	HBAl	HBAl	Hp	HpAl	HpAr	152.35	0.883	0.851
5	HBA	HBAl	HpAl	HpAl	HpAr	152.49	0.915	0.839
6	HBA	HpAl	Hp	Hp	HpAr	152.52	0.909	0.841
7	HBA	HBAl	HpAl	HpAl	HpAr	152.74	0.934	0.831
8	HBA	HBA	HpAl	HpAl	HpAr	152.85	0.920	0.837
9	HBAl	HBAl	HpAl	HpAl	HpAr	153.25	0.912	0.840
10	HBAl	HBAl	Hp	HpAl	HpAl	153.41	0.924	0.835

[a]HBA, hydrogen-bond acceptor; HBAl, hydrogen-bond acceptor aliphatic; Hp, hydrophobic; HpAl, hydrophobic aliphatic; HpAr, hydrophobic aromatic.

The small cost range observed here may be due to two factors, namely molecules in the training set are fairly rigid and have a high degree of structural homology. Due to the relatively small range between the costs for an ideal versus null hypothesis and due moreover to the placement of the identified hypotheses within this range, special care was taken to test for chance correlation. The hypothesis 1 turns out to be the best measure in the test set for the whole training set as attested by the reasonably good correlation between observed and estimated activitities. Hence, the hypothesis 1 was regressed using each molecule in its most chemically reasonable conformation. All test compounds **3**, **8**, **19**, **34**–**36** and **41** were overestimated by hypothesis 1, which had the highest r (0.855) and the smallest RMS. The type of compounds used in preparing Catalyst hypothesis is still limited and it will need improvement to design new molecules.

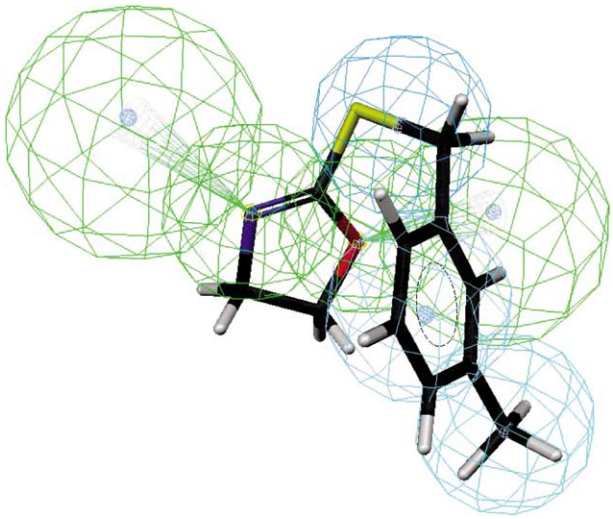

Figure 2. Mapping of **4** onto hypothesis 1, which contains an HBA (green right), an HBAl (green left), an Hp (light blue), an HpAr (blue)

Receptor–Drug Interaction

QSAR modeling is an area of research pioneered by Hansch and Leo,[42] and Hansch and Fujita.[43] QSAR attempts to model the activity of a series of compounds using measured or computed properties of the compounds. More recently, QSAR has been extended by including the three-dimensional information. In drug discovery, it is common to have measured activity data for a set of compounds acting upon a particular protein but not to have knowledge of the three-dimensional structure of the active site. In the absence of such three-dimensional information, one can attempt to build a hypothetical model of the receptor that can provide insight about receptor characteristics. Such a model is known as a Hypo, which provides three-dimensional information about a putative receptor site. Catalyst/Hypo was useful in building 3-D pharmacophore models from the binding activity data and conformational structure. It can be used as an alternative for QSAR methods.

Figure 2 depicts the conformation of the most active SBO **4** in the training set mapped onto the lowest cost hypothesis 1. The molecule maps well onto all five hypotheses features in a similar way in hypotheses 1–10 (data not shown) and therefore these hypotheses are considered to be equivalent. Roughly speaking, hypotheses 1–10 have good similarity in 3-D spatial shape. The phenyl group of **4** overlaps with the HpAr feature of hypothesis 1, whereas the oxygen and nitrogen atoms of oxazolidine ring serve as an HBA and an HBAl, respectively. The Hp feature overlaps neatly with the methyl and the HBAl with methylenethio group, respectively. Thus, the most active OA/TA agonist **4** in the training set maps closely with the statistically most significant hypothesis 1, which is characterized by five features (Fig. 2) and the predicted activity of **4** by hypothesis 1 is reasonable (Table 2). Meanwhile, the oxygen and nitrogen atoms of oxazolidine ring in SBO **10** serve as an HBAl and an HBA, respectively (Fig. 3). The Hp does not fit slightly with the methyl group of **10**, which shows lower activity than **4**. Similarly, the methyl group of **2** dose not overlap with any features of hypothesis 1 (Fig. 4). Thus, the activity of **2** is much lower than **4**. In 2-(arylimino)thiazolidine (AIT) with shorter bridge between phenyl and oxazoline rings than SBO (Fig. 5), the phenyl group of **29** overlaps with the HpAr feature of hypothesis 1, whereas the bridge nitrogen atom serves as an HBA, between a phenyl and thiazolidine rings. However, the HBAl of hypothesis 1 does not fit with **29**, leading to lower inhibitory activity than **4**. The Hp and HpAl features overlap neatly with the two ethyls, respectively. AIO **29** has a phenyl and oxazolidine ring directly connected by nitrogen and thus, is less flexible than SBO **4**, because **29** has less (11) conformational flexibility than that (29) of **4**.

The present studies on OA/TA agonists demonstrate that two HBA sites and three hydrophobic sites located on the molecule seem to be essential in inhibition of pheromone production of *P. interpunctella*. Generally,

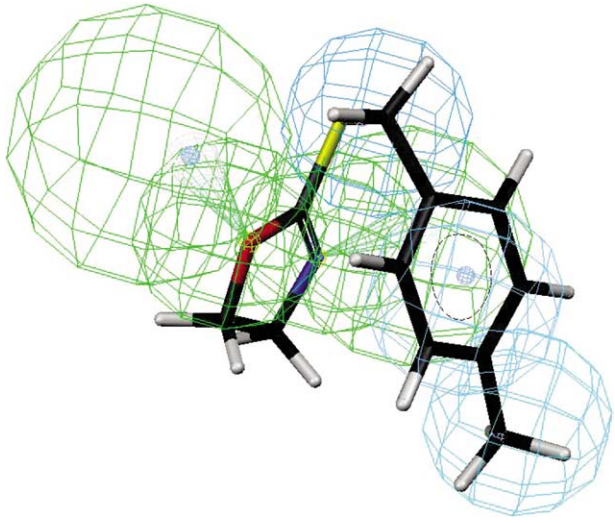

Figure 3. Mapping of **10** onto hypothesis 1, which consists of an HBA (green left), an HBAl (green right), an Hp (light blue), an HpAr (blue) and an HpAl (blue).

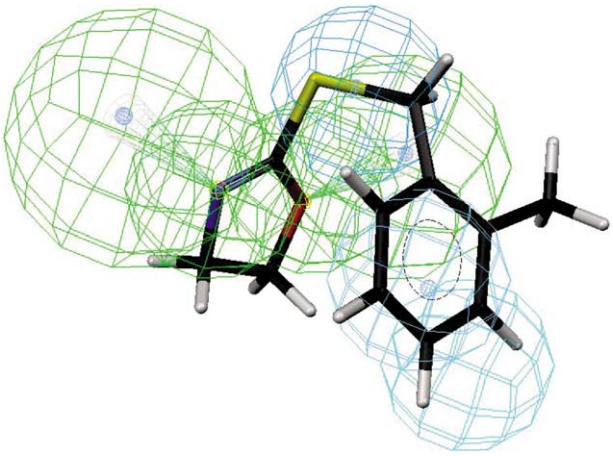

Figure 4. Mapping of **2** onto hypothesis 1, which consists of an HBA (green right), HBAl (green left), an Hp (light blue), an HpAr (blue) and an HpAl (blue).

more active molecules map onto all the features of the hypothesis. Conversely, compounds that are estimated to have low activity map poorly to the hypothesis.[44–47] The predictive character of this five-feature hypothesis was further assessed using candidate molecules, whose structures are shown in Fig. 1, outside of the training set (Table 4). The best statistically significant hypothesis 1 was applied to access the activities of those OA agonists and the predicted values of the molecules are listed in Table 4. It will need improvement to design new molecules. It is necessary to include various types of compounds with variety of activity to obtain better hypothesis and predictions before designing new molecules in the future. The hypothesis 1 is considered to be used in designing new leads for hopefully more active compounds. Further research on the comparison of the 3-D hypotheses from more potent OA/TA agonists as well as those generated from the corresponding data from various insect might be interesting and stimulating

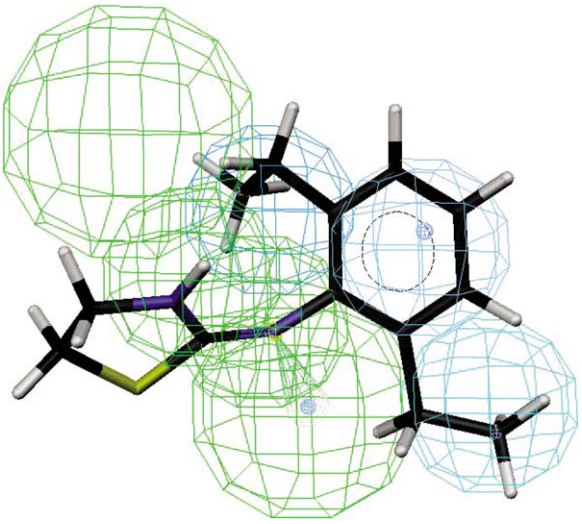

Figure 5. Mapping of **29** onto hypothesis 1, which consists of an HBA (green right), an HBA (green left), an Hp (light blue), an HpAr (blue) and an HpAl (blue).

to investigate further the mechanisms of OA/TA receptor–ligand interactions.

Conclusions

The inhibitors of pheromone production have been reported, which showed also OA-agonist activities.[17] Those OA agonist activities were nonadditive with respect to the activity of a maximally effective concentration of OA.[29] The activities were inhibited by several OA antagonist, the rank-order ability of which to block the OA agonists was identical to the rank-order ability of the same antagonists to block OA. These results suggest that the activities of those compounds are due to their OA-agonist action. Although the inhibitory activities of OA agonists were in μM range for *P. interpunctella,* they were in nM range for *H. armigera*.[48] The result suggests spiecies specificity of the activities, which still remains to be clarified for development of pest-control agents.

Three-dimensional pharmacophore hypotheses were built from a training set of 36 OA/TA agonists. Hypotheses were obtained from this study and applied to map with the active or inactive compounds to explain the mechanism of OA/TA receptor–ligand interactions. Important features were found such as HBA, HBAl, Hp, HpAr and HpAl of the surface-assessable models. Two HBAs and three hydrophobic features are the minimum components of an effective OA/TA agonistic binding hypothesis. Meanwhile, three-dimensional pharmacophore hypotheses were built from a set of 43 agonists against OAR3 in locust nervous tissue.[49] Among the 10 chemical-featured models generated by program Catalyst/Hypo, a hypothesis including an HBA, three Hps and an HpAl features was considered to be important and predictive in evaluating OAR3 agonists. It was found that more active agonists map well onto all the features of the hypotheses, meanwhile for some inactive compounds, their lack of binding affinity is primarily due to their inability to achieve an energetically favorable conformation shared by the active compounds in order to fit the 3-D common feature pharmacophore keys.

Based upon this study, several three-dimensional pharmacophore models for the OA/TA agonists–receptor interactions have been proposed. Those hypotheses are considered to be useful in designing new leads for hopefully more active compounds, although the numbers of compounds tested are still limited. Hence, a further comparison study of 3-D hypothesis models of agonists responsible for the inhibition of sex-pheromone production in *P. interpunctella* is in progress and expected to clarify the mode of action of these compounds acting on the OA/TA receptor. Such work will surely help elucidate the mechanisms of OA/TA receptor–ligand interactions. The above hypotheses studies show that agonists with certain substituents can be potential ligands to OA/TA receptors. They may help to point the way towards developing extremely potent and relatively specific OA/TA agonists, leading to potential pest-con-

Table 4. Predicted activity of OA/TA agonists from hypothesis 1

Compound	Conf.	ID_{50} (mM)		Error
		Experimental	Predicted	
3	28	50	22	−2.2
18	4	50	44	−1.1
19	2	50	38	−1.3
34	53	50	27	−1.9
35	42	50	9.8	−5.1
36	19	50	25	−2.0
41	15	50	29	−1.7

Conf., number of conformational models. In case predicted activity is overestimated, error is obtained by calculating experimental activity divided by predicted value and indicated by minus.

trol agents. In order to optimize the activities of these compounds as OA/TA agonists, more detailed experiments are in progress.

Experimental

Synthesis of OA/TA agonists

The compounds reported here have been prepared according to the ref 17. SBOs **1**–**13** were prepared from oxazolidine-2-thione and substituted benzylamine in the presence of sodium hydride. 2-(Arylimino)oxazolidines (AIOs) **14**–**24** were obtained by cyclodesulfurizing the corresponding thiourea with yellow mercuric oxide. AITs **25**–**30** and 2-(substituted benzylamino)-2-thiazolines (BATs) **31**–**33** were synthesized by cyclization of the corresponding thiourea with concd hydrochloric acid. 2-(2,6-Diethylphenylimino)imidazolidine (AII) **37** was prepared by refluxing the corresponding aniline and 1-acetyl-2-imidazolidone in phosphoryl chloride followed by hydrolysis. 2-(3-methyl benzylthio)-2-oxazine (BOA) **38** was prepared from oxazine-2-thione and *m*-methyl benzylamine in the presence of sodium hydride. 2-(Cinnamylthio)-2-oxazoline (CAO) **39** was prepared from oxazolidine-2-thione and cinnamylamine in the presence of sodium hydride. 2-(2,6-Diethylphenylimino)piperidine (DIP) **41** was obtained by refluxing δ-valerolactam and the corresponding aniline in phosphoryl chloride. 4*H*-Quinazolin-4-one derivative (HQO) **42** was obtained from SBO and *o*-aminobenzoic acid in the presence of sodium hydride. The structures of the compounds were confirmed by ^{1}H and ^{13}C NMR measured with a JEOL JNM-EX400 spectrometer at 400 MHz, tetramethyl silane (TMS) being used as an internal standard for ^{1}H NMR and by elemental analytical data. Chlordimeform (CDM, 96% pure) **40** was a gift from Nihon Nohyaku Co. Ltd. (Osaka, Japan) and used after purification by column chromatography on silica gel.

Insect culture

The colony of *P. interpunctella* was raised on a diet of 80% ground rice, 10% glycerin, 5% brewer's yeast and 5% honey at 28 °C and 70% RH in a 14:10 (light/dark) photoperiod as reported previously.[50] Larvae of wandering stage were pupated between pieces of paper carton and the resulting pupae were sexed and males and females were emerged separately. Emerged virgin females were staged according to age.

In vitro pheromone-production bioassay

Compounds were tested for inhibitory specificity using a modified radiochemical bioassay to monitor de novo pheromone production.[17] Abdominal tips, containing the eighth and ninth abdominal segments with the attached intersegmental membrane, were removed from 1-day-old virgin females under sterile conditions during the first-third h scotophase, using a dim red light for illumination. After preincubation in Pipes-buffered incubation medium[48] for 30 min, the intersegments were dried on tissue paper and then transferred individually to 10 μL medium containing 0.5 μCi [1-^{14}C]acetate in the presence or absence of 0.5 μM synthetic Hez-PBAN and test compounds. All incubations for pheromone production were performed at room temperature, maintaining the photoperiod. After the required incubation period (3 h) in order to measure the incorporation of [1-^{14}C]acetate into pheromone components, the glands were extracted in hexane, which was washed with water, and the amount of radioactivity of the hexane extract was measured using a liquid scintillation counter (LSC, Beckman LS 6500 multipurpose liquid scintillation analyzer) after adding scintillation cocktail (Clearsol I). ID_{50}s were calculated by a sigmoidal curve-fitting program designed for log dose-probit activity analyses using a Macintosh personal computer system.

Computational details

Hypothesis generation. All calculation was conducted on a Silicon Graphics O2, runnning under the IRIX 6.5 operating system. Hypotheses generation and its functionality is available as part of Catalyst/Hypo modeling environment from Accelyrs (San Diego, USA). Molecules were edited using the Catalyst 2D/3-D visualizer. The Catalyst model treats molecular structures as templates consisting of strategically positioned chemical functions that will bind effectively with complementary functions on receptors. The biologically most important functions are deduced from a set of compounds that cover a broad range of activity. Catalyst automatically generated conformational models for each compound using the Poling Algorithm.[38–40] Diverse conformational models for each compound were generated such that the conformers covered accessible conformational space defined within 20 kcal of the estimated global minimum. The models emphasized a conformational diversity under the constraint energy threshold above the estimated global minimum based on use of the CHARMm force field.[38–41] Molecular flexibility is taken into account by considering each compound as a collection of conformers representing a different area of conformational space accessible to the molecule within a given energy range. Catalyst provides two types of conformational analysis: fast and best quality. Fast option was used, specifying 250 as the maximum number of conformers.

The molecules associated with their conformational models was submitted to Catalyst hypothesis generation. The present work shows how a set of various OA/TA agonists, responsible for the inhibition of sex-pheromone production in *P. interpunctella,* may be treated statistically to uncover the molecular characteristics which are essential for high activity. These characteristics are expressed as chemical features disposed in three-dimensional space and are collectively termed a hypothesis. Hypotheses approximating the pharmacophore are described as a set of features distributed within a 3-D space. This process only considered surface accessible functions such as HBA, HBAl, hydrogen-bond donor (HBD), Hp, HpAr, HpAl, negative charge, positive charge, ring aromatic (RA), negative ionizable (NI) and positive ionizable (PI).[51] A preparative test was performed with these features. NI and PI were used rather than negative charge and positive charge in order to broaden the search for deprotonated and protonated atoms or groups at physiological pH. Furthermore, in order to emphasize the importance of an aromatic group corresponding to the phenol moiety of test compounds, RA which consists of directionality was chosen to be included in the subsequent run. The hypothesis generator was restricted to select only five features due to the molecule's flexibility and functional complexity. For molecules larger than dipeptides, Catalyst often will find five-feature hypotheses automatically, but for smaller molecules, three- or four-feature hypotheses might be in the majority. Since hypotheses with more features are more likely to be stereospecific and generally more restrictive models, the total features min value was set to 5 in order to force Catalyst to search for five-feature hypotheses.[32]

Validation of the hypothesis. During a hypothesis generation run, Catalyst considers and discards many thousands of models. It attempts to minimize a cost function consisting of two terms. One penalizes the deviation between the estimated activities of the training set molecules and their experimental values. The other penalizes the complexity of the hypothesis. The overall assumption used is based on Occam's razor, that between otherwise equivalent alternatives, the simplest model is best. Simplicity is defined using the minimum description length principle from information theory. The overall cost of a hypothesis is calculated by summing the cost function consisting of three terms (weight cost, error cost, and configuration cost). Weight cost is a value that increases in a Gaussian form as the feature weight in a model deviates from an idealized value of 2.0. Error cost is a major value that increase as RMS difference between estimated and measured activities. It is obtained by calculating predicted activity divided by experimental value, when predicted activity is underestimated. In case predicted activity is overestimated, it is obtained by calculating experimental activity divided by predicted value and indicated by minus. Configuration cost is a fixed cost which depends on the complexity of the hypothesis, equal to entropy of the hypothesis space.

Besides providing a numerical score for each generated hypothesis, Catalyst provides two numbers to help the chemist assess the validity of a hypothesis. One is the cost of an ideal hypothesis, which is a lower bound on the cost of the simplest possible hypothesis that still fits the data perfectly. The other is the cost of the null hypothesis, which presumes that there is no statistically significant structure in the data, and that the experimental activities are normally distributed about their mean. Generally, the greater the difference between the two costs, the higher the probability for finding useful models. In terms of hypothesis significance, a generated hypothesis with a cost that is substantially below that of the null hypothesis is likely to be statistically significant and bears visual inspection.[52]

Acknowledgements

We thank Dr. Ada Rafaeli (Department of Stored Products, Pheromone Research Lab, Volcani Centre, Israel) for valuable suggestions in rearing *P. interpunctella*. This work was supported in part by a Grant-in-Aid for Scientific Research from the Ministry of Education, Science and Culture of Japan.

References and Notes

1. Raina, A. K. *Ann. Rev. Entomol.* **1993**, *38*, 329.
2. Ma, P. W. K.; Roelofs, W. *Insect Biochem. Molec. Biol.* **1995**, *25*, 467.
3. Rafaeli, A.; Gileadi, C. *Invert. Neurosci.* **1997**, *3*, 223.
4. Jurenka, R. A. *Arch. Insect Biochem. Physiol.* **1996**, *33*, 245.
5. Soroker, V.; Rafaeli, A. *Insect Biochem.* **1989**, *19*, 1.
6. Rafaeli, A.; Soroker, V.; Kamensky, B.; Raina, A. K. *J. Insect Physiol.* **1990**, *36*, 641.
7. Arima, R.; Takahara, K.; Kadoshima, T.; Numazaki, F.; Ando, T.; Uchiyama, M.; Nagasawa, H.; Kitamura, A.; Suzuki, A. *Appl. Entomol. Zool.* **1991**, *26*, 137.
8. Jurenka, R. A.; Jacquin, E.; Roelofs, W. L. *Proc. Natl. Acad. Sci. U.S.A.* **1991**, *88*, 8621.
9. Fonagy, A.; Matsumoto, S.; Schoofs, L.; Loof, A.; De Mitsui, T. *Biotech. Biochem.* **1992**, *56*, 1692.
10. Matsumoto, S.; Ozawa, R.; Nagamine, T.; Kim, G.-H.; Uchiumi, K.; Shono, T.; Mitsui, T. *Biosci. Biotech. Biochem.* **1995**, *59*, 560.
11. Rafaeli, A.; Gileadi, C. *Insect Biochem. Mol. Biol.* **1995**, *25*, 827.
12. Rafaeli, A.; Gileadi, C. *Insect Biochem. Mol. Biol.* **1996**, *26*, 797.
13. Rafaeli, A.; Gileadi, C.; Fan, Y.; Meixun, C. *J. Insect Physiol.* **1997**, *43*, 261.
14. Kuwahara, Y.; Kitamura, C.; Takahashi, S.; Hara, H.; Ishii, S.; Fukami, H. *Science* **1971**, *171*, 801.
15. Brady, U. E.; Tumlinson, J. H.; Brownlee, R. G.; Silverstein, R. M. *Science* **1971**, *171*, 802.
16. Zhu, J.; Ryne, C.; Unelinus, C. R.; Valeur, P. G.; Lofstedt, C. *Entomol. Exp. Appl.* **1999**, *92*, 137.
17. Hirashima, A.; Eiraku, T.; Watanabe, Y.; Kuwano, E.; Taniguchi, E.; Eto, M. *Pest Manag. Sci.* **2001**, *57*, 713.
18. Axelrod, J.; Saavedra, J. M. *Nature* **1977**, *265*, 501.
19. Evans, P. D. In *Reviews in Comparative Molecular Neurobiology*; Heller, S. R., Ed.; Birkhäuser: Basel, 1993; p 287.
20. Evans, P. D. In *Reviews in Comprehensive Insect Physiology Biochemistry Pharmacology*, Kerkut, G. A., Gilbert, G., Eds.; Pergamon: Oxford, 1985; Vol. 11, p 499.
21. Nathanson, J. A. *Mol. Pharm.* **1985**, *28*, 254.
22. Evans, P. D. *J. Physiol.* **1981**, *318*, 99.
23. Roeder, T.; Nathanson, J. A. *Neurochem. Res.* **1993**, *18*, 921.

24. Roeder, T.; Gewecke, M. *Biochem. Pharm.* **1990**, *39*, 1793.
25. Roeder, T. *Life Science* **1992**, *50*, 21.
26. Roeder, T. *Br. J. Pharm.* **1995**, *114*, 210.
27. Roeder, T. *Eur. J. Pharm.* **1990**, *191*, 221.
28. Jennings, K. R.; Kuhn, D. G.; Kukel, C. F.; Trotto, S. H.; Whiteney, W. K. *Pest. Biochem. Physiol.* **1988**, *30*, 190.
29. Hirashima, A.; Yoshii, Y.; Eto, M. *Pestic. Biochem. Physiol.* **1992**, *44*, 101.
30. Ismail, S. M. M.; Baines, R. A.; Downer, R. G. H.; Dekeyser, M. A. *Pest. Sci.* **1996**, *46*, 163.
31. Robertson, H. A.; Juorio, A. V. *Int. Rev. Neurobiol.* **1976**, *19*, 173.
32. Hirashima, A.; Shinkai, K.; Pan, C.; Kuwano, E.; Taniguchi, E.; Eto, M. *Pest. Sci.* **1999**, *55*, 119.
33. Pan, C.; Hirashima, A.; Tomita, J.; Kuwano, E.; Taniguchi, E.; Eto, M. *Internet J. Sci.-Biol. Chem.* **1997**, *1* (http://www.netsci-journal.com/97v1/97013/index.htm).
34. Hirashima, A.; Pan, C.; Tomita, J.; Kuwano, E.; Taniguchi, E.; Eto, M. *Bioorg. Med. Chem.* **1998**, *6*, 903.
35. *Catalyst Tutorial*, Version 4.0; Molecular Simulations Inc.: San Diego, CA, 1998.
36. Pan, C.; Hirashima, A.; Kuwano, E.; Eto, M. *J. Mol. Model.* **1997**, *3*, 455.
37. Hirashima, A.; Pan, C.; Kuwano, E.; Taniguchi, E.; Eto, M. *Bioorg. Med. Chem.* **1999**, *7*, 1437.
38. Smellie, A.; Teig, S. L.; Towbin, P. *J. Comp. Chem.* **1994**, *16*, 171.
39. Smellie, A.; Kahn, S. D.; Teig, S. L. *J. Chem. Inf. Comp. Sci.* **1995**, *35*, 285.
40. Smellie, A.; Kahn, S. D.; Teig, S. L. *J. Chem. Inf. Comp. Sci.* **1995**, *35*, 295.
41. Brooks, B. R.; Brucolleri, R. E.; Olafson, B. D.; States, D. J.; Swaminathan, S.; Karplus, M. *J. Comput. Chem.* **1983**, *4*, 187.
42. Hansch, C.; Leo, A. In *Exploring QSAR: Fundamentals and Applications in Chemistry and Biochemisry*; American Chemical Society: Washington, DC, 1995.
43. Hansch, C.; Fujita, T. *J. Am. Chem. Soc.* **1964**, *86*, 1616.
44. Hirashima, A.; Rafaeli, A.; Gileadi, C.; Kuwano, E. *J. Mol. Graphics Mod.* **1999**, *17*, 43.
45. Hirashima, A.; Morimoto, M.; Kuwano, E.; Taniguchi, E.; Eto, M. *Bioorg. Med. Chem.* **2002**, *10*, 117.
46. Hirashima, A.; Eiraku, T.; Shigeta, Y.; Kuwano, E.; Taniguchi, E.; Eto, M. *Internet Electron. J. Mol. Des* **2002**, *1*, 37 (hyttp://www.biochempress.com).
47. Hirashima, A.; Morimoto, M.; Ohta, H.; Kuwano, E.; Taniguchi, E.; Eto, M. *Int. J. Mol. Sci.* **2002**, *3*, 56 (http://www.biochempress.com).
48. Rafaeli, A.; Gileadi, C.; Hirashima, A. *Pestic. Biochem. Physiol.* **1999**, *65*, 194.
49. Hirashima, A.; Pan, C.; Kuwano, E.; Taniguchi, E.; Eto, M. *Bioorg. Med. Chem.* **1999**, *7*, 1437.
50. Rafaeli, A.; Gileadi, C. *J. Stored Prod. Res.* **1995**, *31*, 243.
51. Greene, J.; Kahn, S.; Savoj, H.; Sprague, P.; Teig, S. *J. Chem. Inf. Comput. Sci.* **1994**, *34*, 1297.
52. Hoffmann, R.; Bourguignon, J.-J. In *Complete Listing of Case Studies by Application Area*; Molecular Simulations Inc. (http://www.msi.com/solutions/cases/notes/CCKB_Peb_full.html).